Paper No.
11375

NACE INTERNATIONAL CORROSION 2011 CONFERENCE & EXPO

Water Chemistry for Corrosion Prediction in High Pressure CO_2 Environments

Mohd F. Mohamed, Azmi M. Nor, Muhammad F. Suhor,
Marc Singer, Yoon Seok Choi and Srdjan Nešić

Institute for Corrosion and Multiphase Technology
Ohio University
Athens, OH 45701
USA

ABSTRACT

Transportation of hydrocarbons accompanied by a liquid or supercritical CO_2 phase has recently become a significant concern in the oil and gas industry particularly as related to exploitation of high CO_2 content gas-fields. The issue of internal line corrosion under such condition has a much broader relevance – it is applicable in the field of enhanced oil recovery as well as CO_2 sequestration and transportation.

Many different CO_2 corrosion models can predict worst case corrosion rates of mild steel in the CO_2 partial pressure range up to 10 bar, however they grossly overestimate the corrosion rates as the partial pressure gets higher. One important first step in understanding the corrosion mechanisms of mild steel in high CO_2 content environments is to develop methods to predict the corresponding water chemistry. The present study focuses on modeling and model validation of water chemistry in the presence of large amounts of CO_2, with partial pressure varying up to 100 bar and temperature up to 100^{o}C, covering gas, liquid and supercritical phases of CO_2.

Keywords: Supercritical CO_2, thermodynamic modeling, CO_2 corrosion prediction model

INTRODUCTION

Many corrosion prediction models for CO_2 corrosion have been developed over the last four decades. Most of these models can successfully predict the corrosion rates in environments where partial pressure of CO_2 is up to 10 bar. However, the ability of these models to predict corrosion rates beyond 10 bar of CO_2 is brought into question. If we briefly recall that the CO_2 corrosion prediction modeling began in the 1970's with de Waard and coworkers[1,2] who developed simple equations and the first nomogram which was extensively used in the oil and gas industry, especially for material selection and design. Gray et al. and Nesic et al. presented a more elaborate mechanistic CO_2 corrosion prediction models and mechanisms of CO_2 corrosion in their papers from 1989, 1990 and 1996 [3,4,5]. One of the strengths of a mechanistic modeling approach is its flexibility in extending the validity domain without recursive recalibration of all parameters, i.e., it is easy to add new knowledge or account for the influence of new parameters without a major modification of the existing model structure[6].

The main objective of this work is to develop a water chemistry model valid in high CO_2 partial pressure environments and to incorporate it into a mechanistic approach to predict corrosion rates of mild steel. More specifically, the work presented below was structured into two main tasks:

- Acquire a good understanding of the homogenous chemical reactions involved in a H_2O-CO_2 system and build a thermodynamic model based on the information available in the open literature.
- Develop an experimental set-up that enables the study of water chemistry at high CO_2 partial pressures and validate the model with the experimental data.

THEORETICAL BACKGROUND AND MODELING

It is assumed that the main homogenous chemical reactions involved in a H_2O-CO_2 system are basically the same, whatever the partial pressure of CO_2. These reactions are listed below:

- Water dissociation $H_2O_{(l)} \longleftrightarrow H^+_{(aq)} + OH^-_{(aq)}$
- Carbon dioxide dissolution $CO_{2(g)} \leftrightarrow CO_{2(aq)}$
- Carbon dioxide hydration $CO_{2(aq)} + H_2O_{(l)} \longleftrightarrow H_2CO_{3(aq)}$
- Carbonic acid dissociation $H_2CO_{3(aq)} \longleftrightarrow H^+_{(aq)} + HCO^-_{3(aq)}$
- Bicarbonate ion dissociation $HCO^-_{3(aq)} \longleftrightarrow H^+_{(aq)} + CO^{2-}_{3\ (aq)}$

What differs between low and high pressure is the non-ideality of the solution in the latter case, which needs to be reflected by the choice of equations used to represent the equilibrium constants governing each of these chemical reactions.

In the present work, the equilibrium constants for high pressure CO_2 above 10 bar were found in the open literature and implemented. Most significant previous experimental and theoretical studies related to water chemistry in high partial pressure CO_2 environments which were used are Meyssami et al[7], Duan & Li[8] and Spycher et. al[9]. Most of the constants were taken from

Spycher (2003)[9], Duan & Li (2008)[8] and Palmer & Van Eldik [10]. The constants from Spycher et al. are valid for CO_2-water system in the temperature range of 12-100^oC and pressures up to 600 bar, whereas the constants from Duan & Li 2008 are valid at 1-100^oC and pressures up to 2000 bar.

When implemented the water chemistry model can provide the concentrations of aqueous species such as: dissolved CO_2, H_2CO_3, H^+, OH^-, HCO_3^- and CO_3^{2-}. Once concentrations of these species are known in bulk solution, they are an important input for predictions of the corrosion rate, protective film formation, etc. For example the H_2CO_3 and H^+ species are the main oxidizing agents in corrosion of mild steel in H_2O-CO_2.environments.

In the following text, the various chemical reactions described above are analyzed and their validity extended to high partial pressures of CO_2

Dissolution of Carbon Dioxide

The dissolution of carbon dioxide in water at high CO_2 partial pressures of is different from that at low CO_2 partial pressures due to the non-ideality of the phases. In low pressure CO_2 systems, the concentration of dissolved CO_2 is directly proportional to its partial pressure. The solubility constant is calculated using the Henry's law which is as applicable as the concentration of dissolved CO_2 is relatively small.

$$CO_2(g) \overset{Ksol}{\Leftrightarrow} CO_2(aq) \tag{1}$$

$$K_{sol} = \frac{C_{CO_2(aq)}}{P_{CO_2(g)}} \tag{2}$$

where C_{CO_2} represents the concentration of CO_2 dissolved in water, and p_{CO_2} represents the partial pressure of carbon dioxide. The unit for the solubility constant is mol/(liter*bar).

In high pressure CO_2 systems, however, the relationship between concentration and pressure is no longer linear and Henry's law cannot be used. Instead, the non-ideality of the gas phase must be taken into account using the following equations[9]:

$$y_{H_2O} = \frac{K^o_{H_2O}\left(1 - x_{CO_2}\right)}{\phi_{H_2O} P_{Tot}} \exp\left(\frac{\left(P - P^o\right)\overline{V}_{H_2O}}{RT}\right) \tag{3}$$

$$x_{CO_2} = \frac{\phi_{CO_2}\left(1 - y_{H_2O}\right)P_{Tot}}{55.508 K^o_{CO_2(g)}} \exp\left(-\frac{\left(P - P^o\right)\overline{V}_{CO_2}}{RT}\right) \tag{4}$$

where y_{H_2O} and x_{CO_2} represent the mole fraction of water in the CO_2 phase and the mole fraction of carbon dioxide in water, respectively.

The equations below are used to calculate the fugacity coefficients of CO_2 (ϕ_{CO_2}) and H_2O (ϕ_{H_2O}).

$$\ln(\phi_{H_2O}) = \ln\left(\frac{V}{V-b_{CO_2}}\right)+\left(\frac{b_{H_2O}}{V-b_{CO_2}}\right)-\left(\frac{2\sum_{i=1}^{n} y_{CO_2}a_{CO_2-H_2O}}{RT^{1.5}b_{CO_2}}\right)\ln\left(\frac{V+b_{CO_2}}{V}\right)$$
$$+\left(\frac{a_{CO_2}b_{H_2O}}{RT^{1.5}b_{CO_2}^2}\right)\left[\ln\left(\frac{V+b_{CO_2}}{V}\right)-\left(\frac{b_{CO_2}}{V+b_{CO_2}}\right)\right]-\ln\left(\frac{PV}{RT}\right) \quad (5)$$

$$\ln(\phi_{CO_2}) = \ln\left(\frac{V}{V-b_{CO_2}}\right)+\left(\frac{b_{CO_2}}{V-b_{CO_2}}\right)-\left(\frac{2\sum_{i=1}^{n} y_{H_2O}a_{CO_2-H_2O}}{RT^{1.5}b_{CO_2}}\right)\ln\left(\frac{V+b_{CO_2}}{V}\right)$$
$$+\left(\frac{a_{CO_2}b_{CO_2}}{RT^{1.5}b_{CO_2}^2}\right)\left[\ln\left(\frac{V+b_{CO_2}}{V}\right)-\left(\frac{b_{CO_2}}{V+b_{CO_2}}\right)\right]-\ln\left(\frac{PV}{RT}\right) \quad (6)$$

The volumes of compressed carbon dioxide gas V_{CO_2} and water V_{H_2O} can be obtained by solving the Redlich-Kwong equation of state. The cubic equation below is then solved using a Newton-Raphson algorithm. The value of a_{CO_2} and $a_{H_2O-CO_2}$ are $6x10^7$ and $7.89x10^7$ accordingly. The value of b_{CO_2} and b_{H_2O} are 27.80 and 18.18. The values are obtained assuming the infinite water dilution in the CO_2-rich phase[4].

$$V^3 - V^2\left(\frac{RT}{P}\right) - V\left(\frac{RTb_{CO_2}}{P} - \frac{a_{CO_2}}{PT^{0.5}} + b_{CO_2}^2\right) - \left(\frac{a_{CO_2}b_{CO_2}}{PT^{0.5}}\right) = 0 \quad (7)$$

where, R=83.1447 bar*cm^3/(mol*K), V is in cm^3/mol, P is in bar, and T is in K.

Once the cubic expression is solved and the values of compressed gas volume are calculated, the carbon dioxide solubility constant is obtained by evaluating each parameter in equations 1 to 7. The values of the constants listed above are available in the original publications[9].

Carbon Dioxide Hydration

The equilibrium constant K_{hy} for the carbon dioxide hydration is obtained from Palmer and Van Eldik[10]. K_{hy} does not change significantly within the temperature range of 20 – 100^{o}C[10]. Since it is not pressure-dependent, the equilibrium constant of carbon dioxide hydration of 2.58 x10^{-3} (which is used in low pCO_2 environment model) is applicable for high CO_2 content.

$$CO_2 + H_2O \overset{Khy}{\Leftrightarrow} H_2CO_3 \quad (8)$$

$$K_{hy} = C_{H_2CO_3} / C_{H_2O}\, C_{CO_2} \quad (9)$$

Carbonic Acid Dissociation

The constant K_{ca} is taken from Duan and Li. The constant is a function of temperature and pressure and can be calculated reliably from 0^{o}C to 100^{o}C and within pressure ranges from 1 to 3000 bar[8].

$$H_2CO_3 \overset{Kca}{\Leftrightarrow} HCO_3^- + H^+ \tag{10}$$

$$K_{ca} = C_{H^+} C_{HCO_3^-} / C_{H_2CO_3} \tag{11}$$

$$\begin{aligned} \ln Kca = {} & 233.5159304 - 11974.38348 \cdot T^{-1} - 36.50633536 \ln T \\ & + (-45.08004597 \cdot T^{-1} + 2131.318848 \cdot T^{-2} + 6.714256299 \cdot T^{-1} \ln T)(P - P_s) \\ & + (0.008393915212 \cdot T^{-1} - 0.4015441404 \cdot T^{-2} - 0.00124018735 \cdot T^{-1})(P - P_s)^2 \end{aligned} \tag{12}$$

where, P_s is saturation pressure of water.

Bicarbonate Anion Dissociation

The K_{bi} can be calculated at various temperatures and pressures and is valid from 0°C to 100°C and from 1 to 3000 bar**[8].**

$$HCO_3^- \overset{Kbi}{\Leftrightarrow} H^+ + CO_3^{2-} \tag{13}$$

$$K_{bi} = C_{H^+} C_{CO_3^{2-}} / C_{HCO_3^-} \tag{14}$$

$$\begin{aligned} \ln K_{bi} = {} & -151.1815202 - 0.088695577T - 1362.259146 \cdot T^{-1} + 27.79798156 \ln T \\ & - (29.51448102 \cdot T^{-1} + 1389.015354 \cdot T^{-2} + 4.419625804 \cdot T^{-1} \ln T)(P - P_s) \\ & + (0.003219993525 \cdot T^{-1} - 0.1644471261 \cdot T^{-2} - 0.0004736672395 \cdot T^{-1} \ln T)(P - P_s)^2 \end{aligned} \tag{15}$$

Water Dissociation

This equation for the equilibrium constant is taken from Duan and Li **[8].**

$$H_2O \overset{Kwa}{\Leftrightarrow} H^+ + OH^- \tag{16}$$

$$K_{wa} = C_{H^+} C_{OH^-} \tag{17}$$

$$\begin{aligned} \log K_{wa} = {} & -4.098 - 3245.2 \cdot T^{-1} + 2.2362 \cdot 10^5 \cdot T^{-2} - 3.984 \cdot 10^7 \cdot T^{-3} + \\ & (13.957 - 1262.3 \cdot T^{-1} + 8.5641 \cdot 10^5 \cdot T^{-2}) \log \rho_{H_2O} \end{aligned} \tag{18}$$

Where ρ_{H_2O} is the density of water in g/cm^3 and T is temperature in K.

Electroneutrality

The electroneutrality of the H_2O–CO_2 system can be described with the following equation:

$$C_{H^+} = C_{OH^-} + C_{HCO_3^-} + 2C_{CO_3^{2-}} \tag{19}$$

EXPERIMENTAL METHODOLOGY AND SET-UP

The present experimental matrix was designed to validate the accuracy of the water chemistry model in a temperature range of up to 100^{o}C and at CO_2 pressures of up to 100 bar.

Three types of experiments were selected for the model validation as follows:

- Solubility of CO_2 in water.
- Solubility of water in CO_2.
- pH of the water.

Solubility of CO_2 in Water

The objective of the experiments was to compare the mole fraction of dissolved CO_2 in water with predicted data. All of the experiments related to the study of the water chemistry were performed in the 20L autoclave pictured in Figure 1.

Figure 1: 20L high pressure autoclave used in this study

The 20 liter autoclave was filled with 10 liters of de-ionized water and CO_2 was added to the required pressure. Care was taken to ensure that the system had reached equilibrium before any measurement was performed. For measurements, 50ml of water was transferred from the high pressure autoclave into the low pressure 500 ml sampling bomb. The sampling bomb was previously purged with CO_2 and its initial pressure was set at 2 bar. The 50 ml liquid sample taken under pressure from the 20L autoclave was then allowed to de-gas and to reach equilibrium. The sampling bomb was designed so that the consequent rise in pressure (and change in temperature) would be relatively small, keeping the overall pressure under 10 bars.

In these conditions, Henry's law could be used to calculate the CO_2 content in the water. The total amount of CO_2 present in the sampling bomb was then evaluated and this enabled the estimation of the amount of dissolved CO_2 initially present in the 50 ml liquid sample taken from the autoclave. The key step in this measurement method was to have a very good control of the volume of the liquid sampled. The schematic diagram for solubility CO_2 in water set-up is shown in Figure 2.

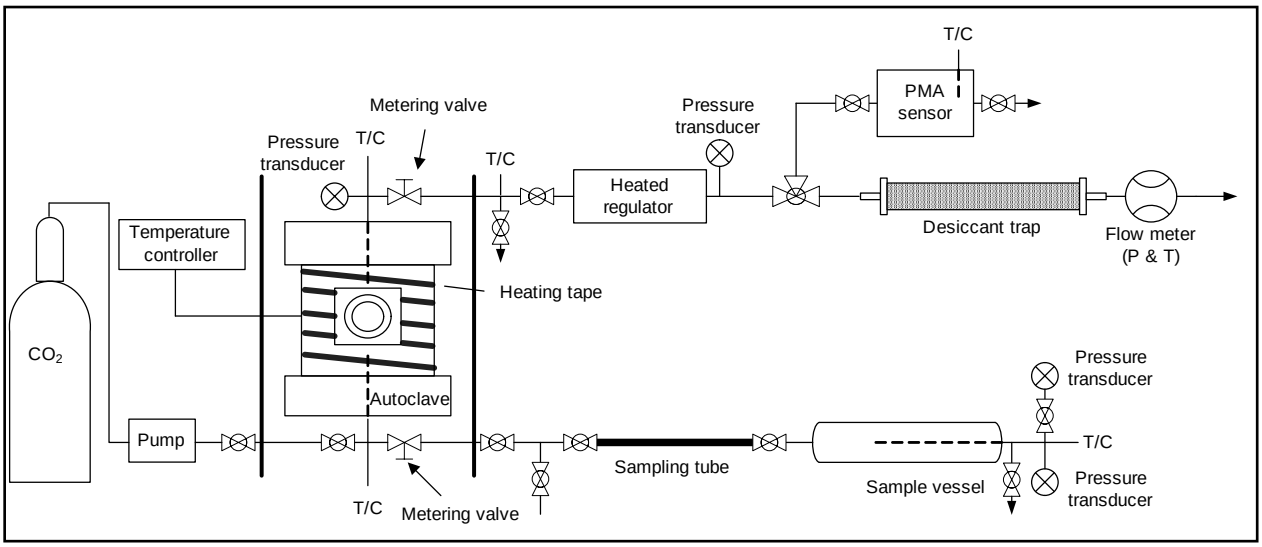

Figure 2: Schematic diagram for the solubility of water in CO_2 and CO_2 in water experimental set-up.

Solubility of Water in CO_2 (yH_2O)

The objective of this part was to determine the mole fraction of water vapor in the CO_2 gas phase. The measured data was compared to predicted data that was developed using equations (1) through (7). The 20L autoclave was filled with 4 liters of deionized water and pressurized. Again, special care was taken that the system had reached equilibrium before any measurement was performed. Any condensation of water vapor due to the pressure drop during sampling was prevented by applying a heating tape along the tubing from the autoclave to the measurement setup.

Two independent methods were used to measure the amount of water vapor in the gas phase: an absolute humidity sensor and a desiccant trap. The screening and selection of measurement techniques for determining water content in the gas phase was reviewed by Yarrison et al.[11]. Figure 2 shows the experimental set-up including the humidity sensor and the desiccant trap.

The idea behind using the humidity sensor method was to bleed and depressurize a small stream of the gas phase (containing water vapor) from the autoclave inside a small vessel equipped with an absolute humidity sensor. The temperature and pressure in the sampling vessel were then recorded. The dew point measurement inside the small vessel was used to back-calculate the molar percentage of water vapor in the gas stream. This method was only valid for temperatures below 60°C, due to the limitations of the sensor.

The desiccant trap method involved the slow bleeding and depressurizing of a small stream of the gas phase (containing water vapor). This stream was passed through a tube full of desiccant material ($CaCl_2$ and a molecular sieve), which trapped the water. A mass flow meter located downstream from the tube measured the dry CO_2 mass flow rate. The molar content of the gas stream was calculated based on the mass change of the desiccant and the totalized CO_2 mass flow rate.

pH of the System

pH measurement is a practical and important way to check if the chemistry of the water/CO_2 solution is modeled properly. A high-pressure glass pH probe and a saturated Ag/AgCl reference electrode were used to measure the concentration of protons (hydronium ions) at three different temperatures and at pressure up to 80 bar, as shown in Figure 3. The pH probe and reference electrode were calibrated at ambient temperature and pressure using buffer solutions at pH 4, 7 and 10. The probe measurement error is ±0.2 unit, as indicated by the probe manufacturer. The 20L autoclave was filled with 4 liters of deionized water and CO_2 was introduced in the vessel and the system was allowed to stabilize until equilibrium was reached. The challenge in such a test was to find a suitable pH probe and a methodology that can be applied in high partial pressure CO_2 environments. The current pH probe proved relatively reliable but was lacking in accuracy.

Figure 3: High pressure glass pH probe and Ag/AgCl reference electrode used to measure proton (hydronium ion) concentration.

RESULTS

The predicted concentration of CO_2, H_2CO_3, HCO_3^- and CO_3^{2-} over partial pressure of CO_2 up to 80 bar is shown in Figure 4 to Figure 7. The concentrations of H_2CO_3 and HCO_3^- present the same trend as the solubility of CO_2 in water, as shown in Figure 4 to Figure 7. That is, the concentrations increased with increasing pressure but decreased with increasing temperature. However, the concentration of CO_3^{2-} increased with increasing pressure and temperature.

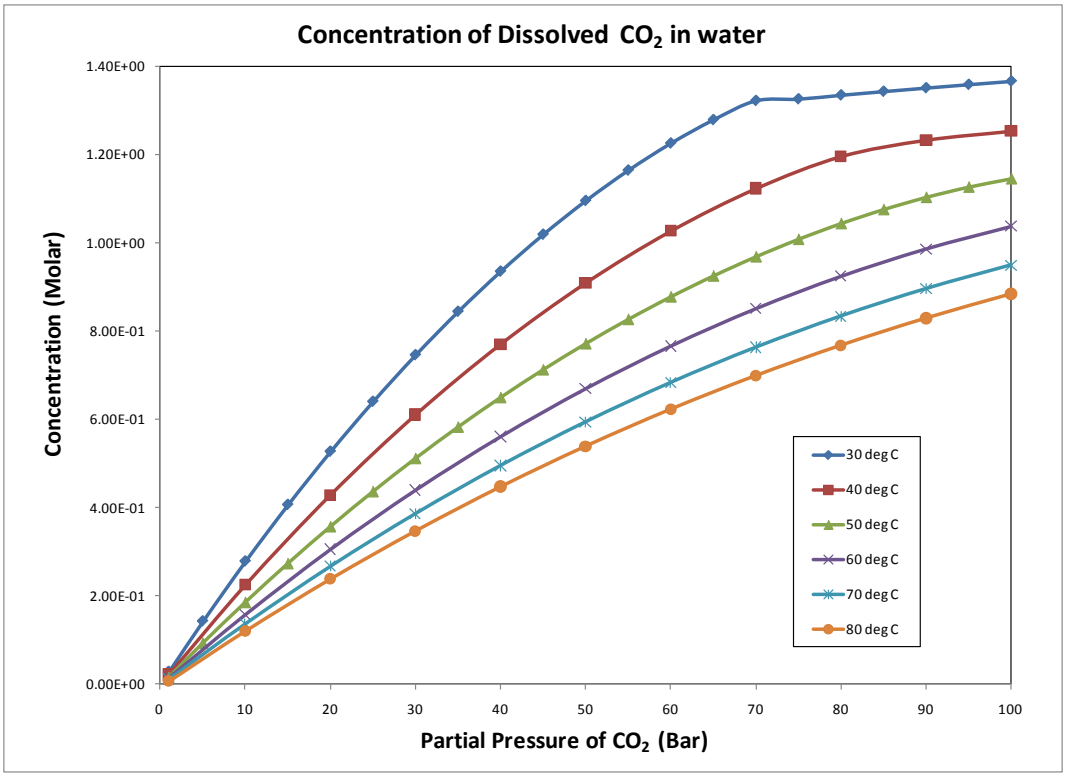

Figure 4: Calculated CO_2 content in water over partial pressure of CO_2.

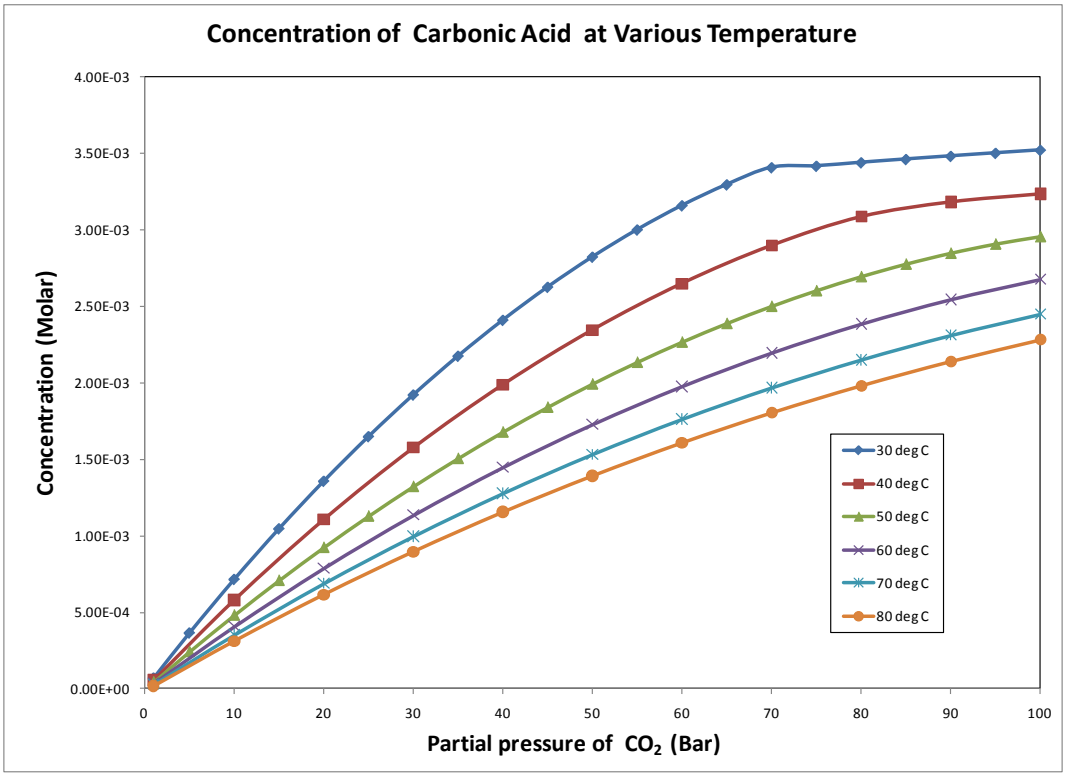

Figure 5: Calculated H_2CO_3 over partial pressure of CO_2.

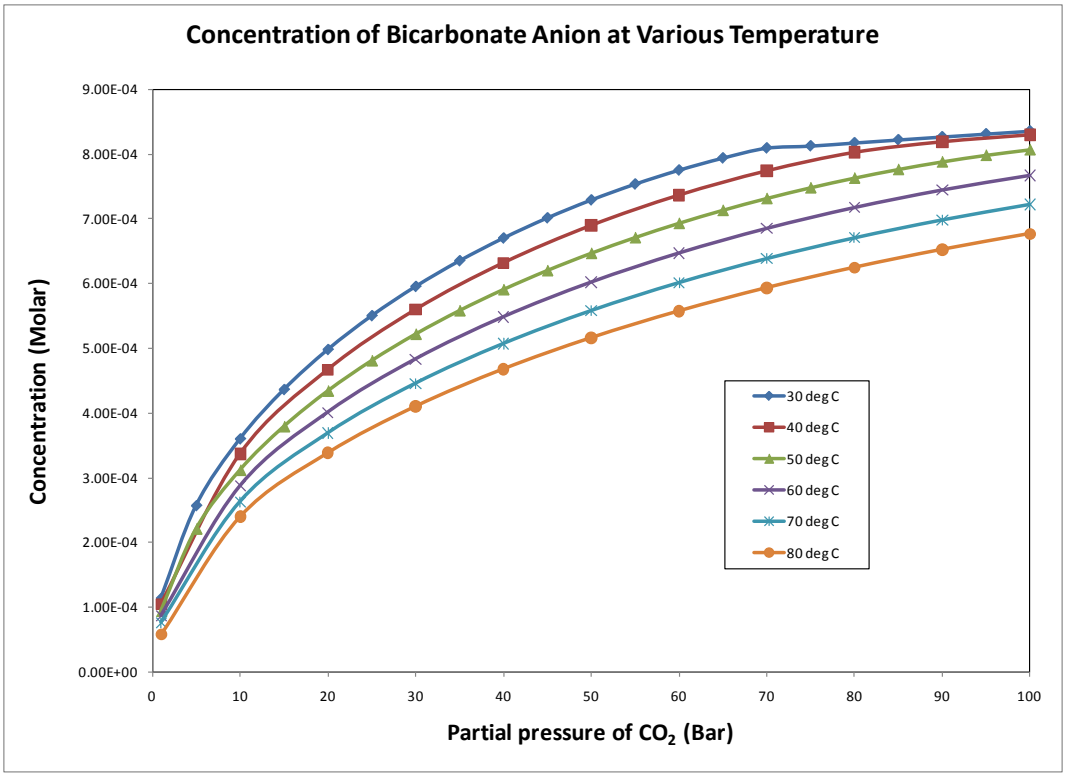

Figure 6: Calculated HCO_3^- over partial pressure of CO_2.

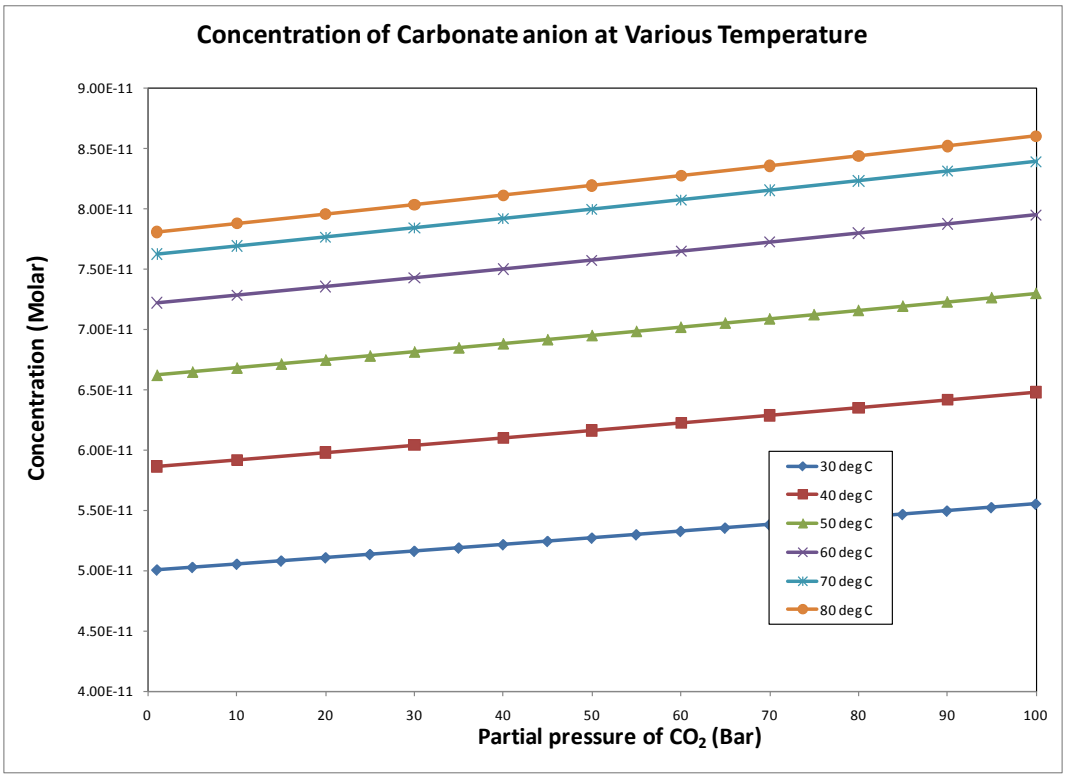

Figure 7: Calculated CO_3^{2-} over partial pressure of CO_2.

Figure 8 to Figure 10 show the experimental data for the solubility of CO_2 in water with mole fraction (x_{CO2}) as a function of CO_2 partial pressure (pressure from 0 to 100 bar at temperatures of 25, 40, and 60^o C, respectively). The results suggest that, at the three temperatures, the amount of dissolved CO_2 increased as the CO_2 partial pressure increased. However, the increase in temperature led to a decrease in x_{CO2}. It must be noted that as temperature increases, the solubility of CO_2 in water deviates further from Henry's Law; that is, the domain of validity of Henry's Law is at best 20 bars at 25^o C, and only 8 bars at 60^o C.
Figure 11 shows the predicted mole fraction of CO_2 in H_2O over partial pressure of CO_2 up to 100 bar. The solubility of water in CO_2 increased with increasing partial pressure of CO_2 and temperature.

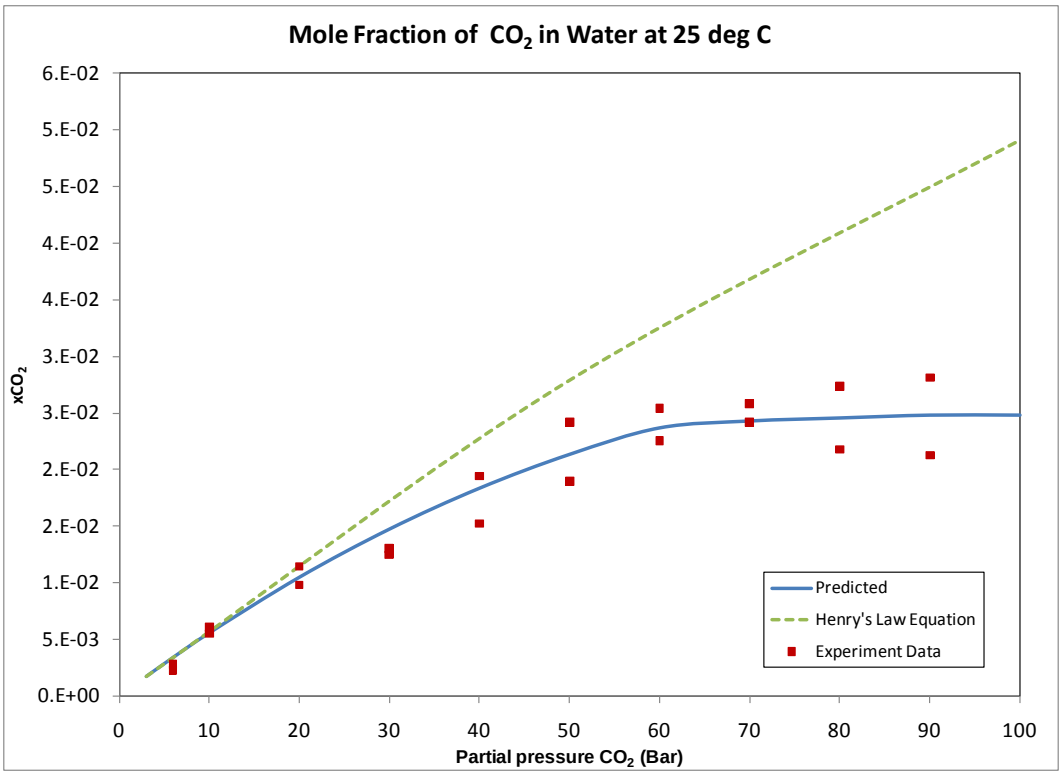

Figure 8: Comparison between experimental results and modeling for the solubility of CO_2 in water at 25°C

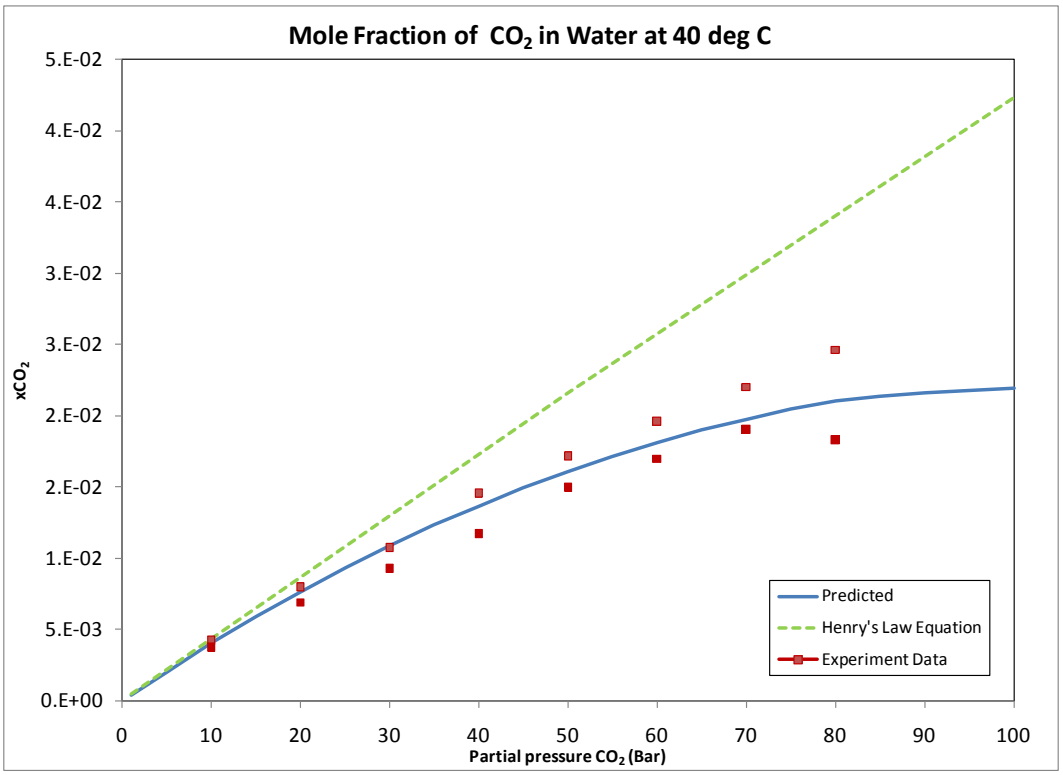

Figure 9: Comparison between experimental results and modeling for the solubility of CO_2 in water at 40°C

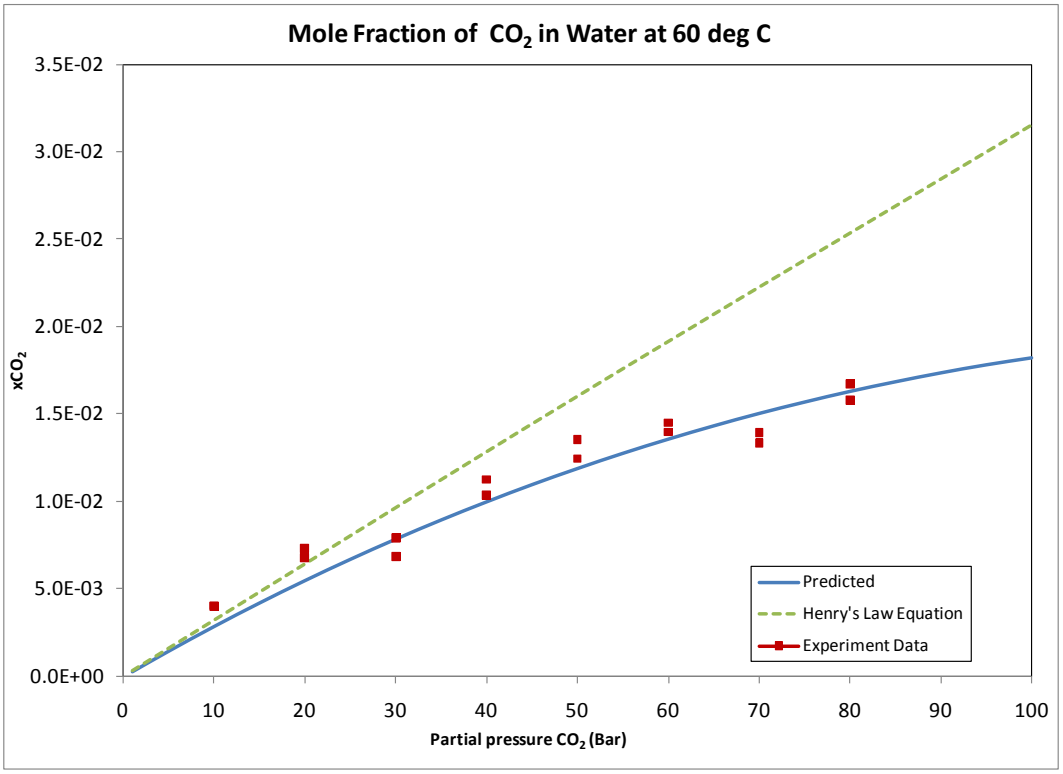

Figure 10: Comparison between experimental results and modeling for the solubility of CO_2 in water at 60°C

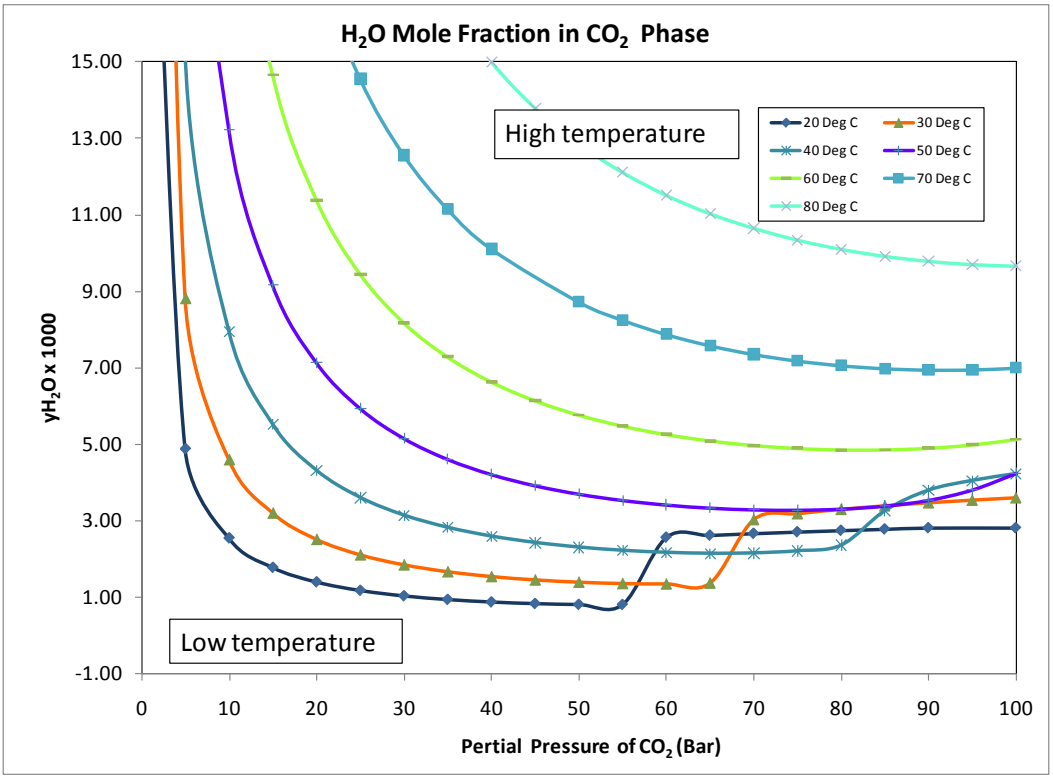

Figure 11: Calculated water content in CO_2 (gas phases).

Figure 12 to Figure 14 show the solubility of water in CO_2 in mole fraction (yH_2O) as a function of CO_2 partial pressure (pressure from 0 to 100 bar and temperature of 25, 40, and 60^o C, respectively). Two types of measurement -- humidity sensor and desiccant traps -- were applied at temperatures of 25^{o}C and 40^{o}C; only the desiccant trap method was applied at 60^{o}C. The figures suggest that at the three temperatures, the amount of water soluble in liquid/supercritical CO_2 phase increases as the CO_2 partial pressure increases. The figures also show that the solubility of water in CO_2 phase increases as the temperature increases.

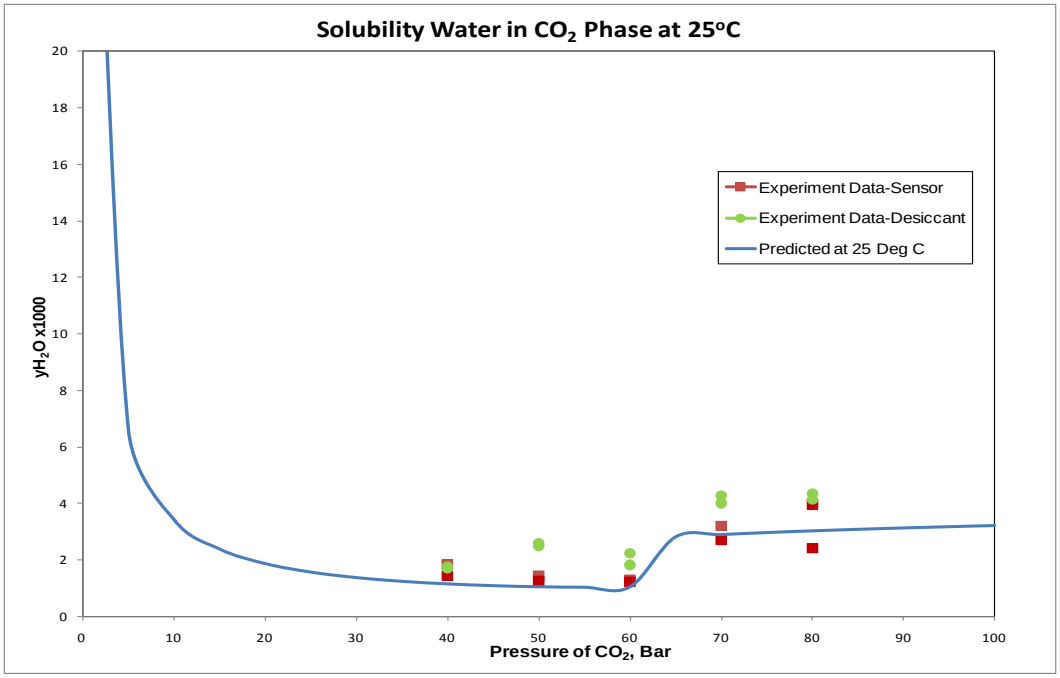

Figure 12: Comparison between experimental results and modeling for the solubility of water in CO_2 at 25°C

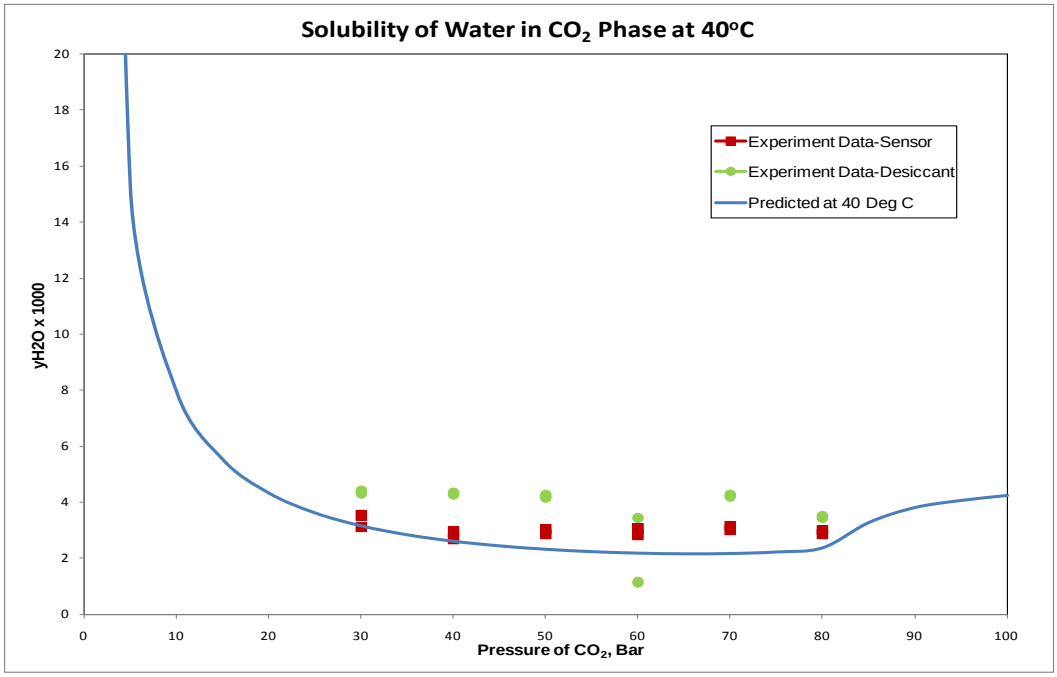

Figure 13: Comparison between experimental results and modeling for the solubility of water in CO_2 at 40°C

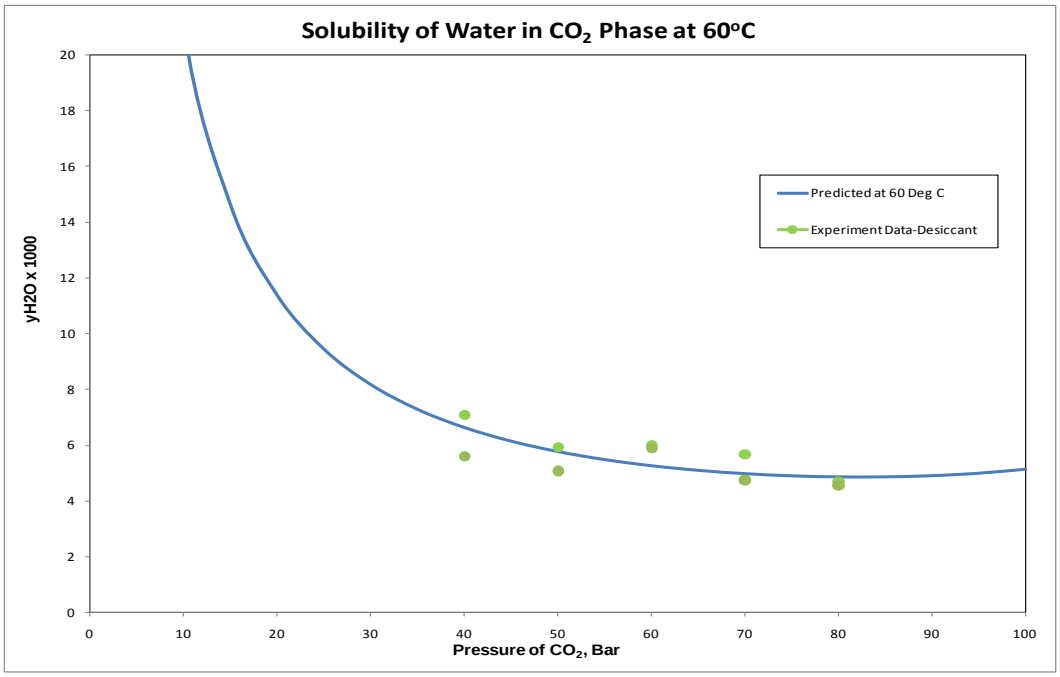

Figure 14: Comparison between experimental results and modeling for the solubility of water in CO_2 at 60°C

Figure 15 to Figure 17 show the pH measurement test as a function of CO_2 partial pressure of 1 to 100 bar at 25°C, 40°C and 60°C, respectively. The results show that pH decreased with increasing partial pressure of CO_2 because the amount of dissolved CO_2 in water increases as

the CO_2 partial pressure increases. However, the increase in temperature led to a decrease in pH. It must be noted that as the temperature increased, a smaller amount of CO_2 was soluble in water.

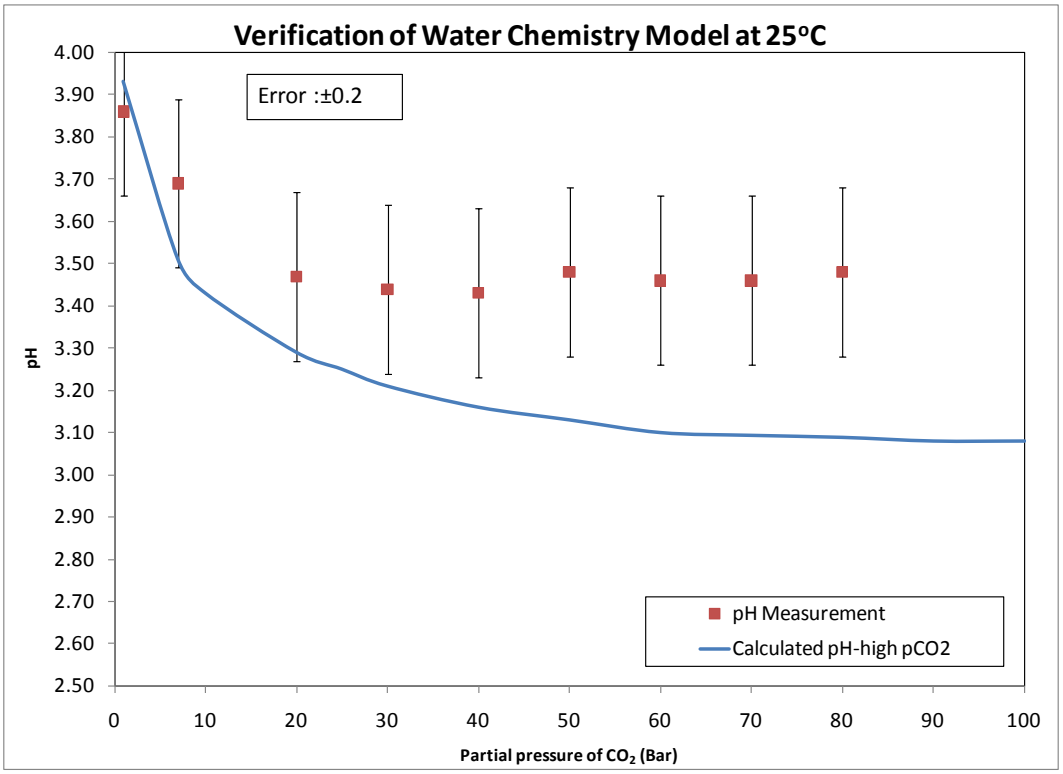

Figure 15: Comparison between pH measurements and modeling results at 25°C

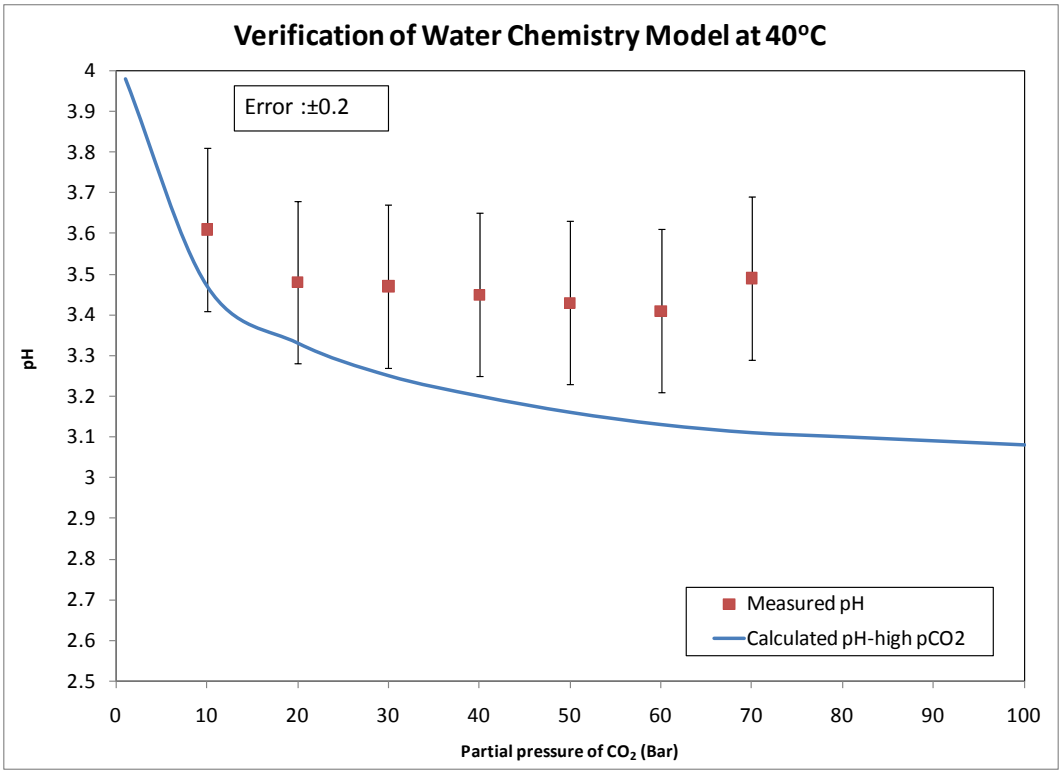

Figure 16: Comparison between pH measurements and modeling results at 40°C

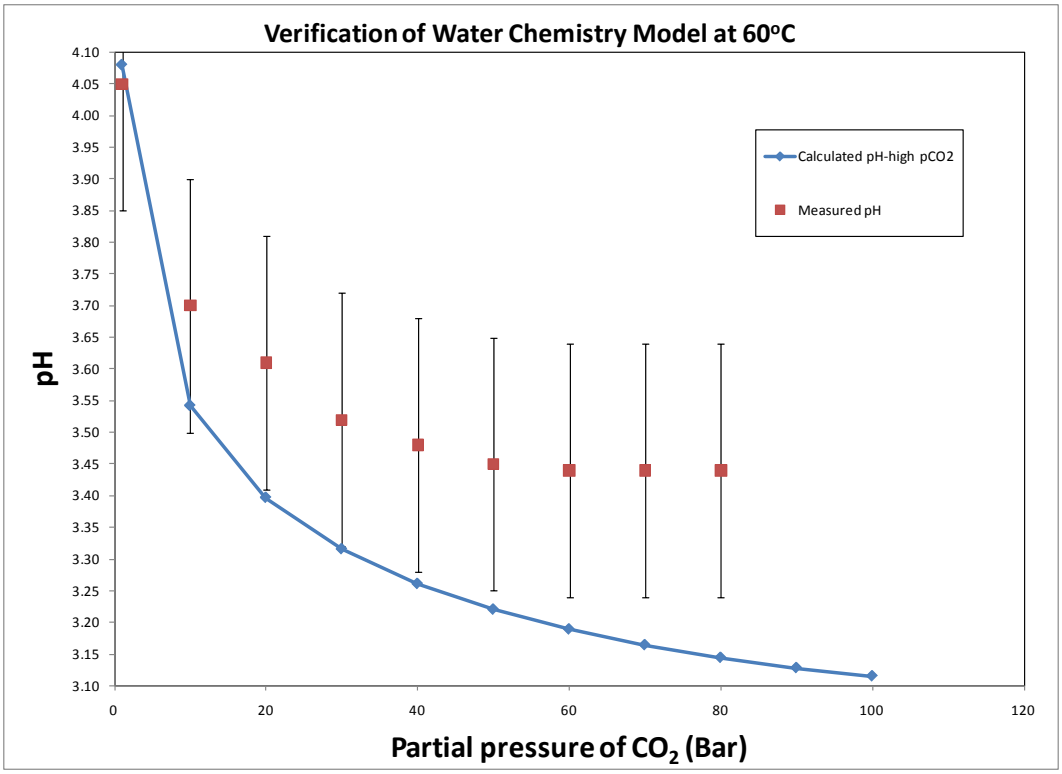

Figure 17: Comparison between pH measurements and modeling results at 60°C

CONCLUSIONS

- The experimental set-up and measurement techniques used in this study were successful in accurately determining the mutual solubility in CO_2-H_2O systems.
- Experimental data obtained in the solubility study agree well with model predictions.
- pH measurements using the high pressure, high temperature pH probe tend to be higher than the simulated data.

ACKNOWLEGMENTS

The authors wish to acknowledge their colleagues at the ICMT and PETRONAS for their technical and financial support and the permission to publish the present paper.

REFERENCES

1. L.G.S Gray, B.G.Anderson. Effect of pH and Temperature on the Mechanism of Carbon Steel Corrosion by Aqueous Carbon Dioxide. *CORROSION/1990, paper no.40.* (Houston, TX: NACE, 1990).

2. L.G.S. Gray, B.G.Anderson. Mechanisms of Carbon Steel Corrosion in Brines Containing Dissolved Carbon Dioxide at pH 4. *CORROSION/1989, paper no. 464.* (Houston, TX: NACE, 1989).
3. Matt Yarrison, Kenneth R. Cox, Walter G Chapman. Measurement and Modeling of the Solubility in Water in Supercritical Methane and Ethane from 310 and 477 K and Pressures from 3.4 to 110 MPa. *Industrial and Engineering Chemistry Research.* 2006, Vol. 46, pp. 6770-6777.
4. N.Spycher, K.Pruess,J Ennis-King. CO_2-H_2O mixtures in the geological sequestration of CO_2. 1. Assessment and calculation of mutual solubulities from 12 to 100^oC and up to 600 bar. *Geochimica et Cosmochimica Acta.* 2003, pp. Vol 67. 3015-3031.
5. Nesic, S. Key issues related to modeling of internal corrosion of oil and gas- A review. *Corrosion Science.* 2007, 49 (4308-4338), pp. 4308-4338.
6. R.V.Eldik, D.A.Palmer. Effects of pressure on the kinetics of the dehydration of carbonic acid and the the hydrolysis of CO_2 in aqueous solution. *Journal of Solution Chemistry.* 1982, Vol. 11, pp. Vol 11. 339-346.
7. S.Nesic, J.Postlethwaite, S.Olsen. An Electrochemical Model for Prediction of Corrosion of Mild Steel in Aqueous Carbon Dioxide Solutions. *Corrosion Science.* April 1996, (Houston, TX: NACE, 1996).
8. Zhenhao Duan, Dedong Li. Coupled phase and aqueous species equilbrium of the H_2O-CO_2-NaCl-$CaCO_3$ systems from 0 to 250 deg C, 1 to 1000 bar with NaCl concentrations up to saturation of halite. *Geochimica et Cosmochimica Acta.* 2008, Vol. 72, 5128-5145.
9. D.Waard, D.Milliams. Carbonic Acid Corrosion of Steel. *Corrosion Journal.* 1975, Vol. 31, 5.
10. D.Waards, D.Milliams. Prediction of Carbonic Acid Corrosion in Natural Gas Pipelines. *First International Conference on the internal and external protection of pipes.* September 1975.
11. Khalifah, Raja G. Carbon Dioxide Hydration Activity of Carbonic Anhydrase: Paradoxical Consequences of the Unusually Rapid Catalysis. *Proceedings of the National Academy of Sciences of the United States of America,.* Vols. Vol. 70, No. 7 (Jul., 1973), pp. 1986-1989.
12. Behrouz Meyssami, Murat O. Balaban, Arthur A. Teixeira. Prediction of pH in Model Systems Pressurized with Carbon Dioxide. *Biotechnology Progress.* 1992, Vol. 8, 149-154.

NOMENCLUTURE

Nomenclature	
K_{sol}	Equilibrium constant for solubility of CO_2 in water, Molar/Bar
K_{hy}	Equilibrium constant for hydration of CO_2, per second
K_{ca}	Equilibrium constant for dissociation of H_2CO_3 , $Kmol/m^3$
K_{bi}	Equilibrium constant for dissociation of HCO_3^- , $Kmol/m^3$
K_{wa}	Equilibrium constant for dissociation of water , $Kmol/m^3$
C_{CO_2}	Concentration of CO_2 in bulks solution, $Kmol/m^3$
$C_{H_2CO_3}$	Concentration of H_2CO_3 in bulks solution, $Kmol/m^3$
$C_{HCO_3^-}$	Concentration of HCO_3^- in bulks solution, $Kmol/m^3$
$C_{CO_3^{2-}}$	Concentration of CO_3^{2-} in bulks solution, $Kmol/m^3$
C_{H^+}	Concentration of H^+ in bulks solution, $Kmol/m^3$
C_{OH^-}	Concentration of OH^- in bulks solution, $Kmol/m^3$
P_{CO_2}	Partial pressure of CO_2 in bar.
P_{H_2O}	Partial pressure of water in bar.
y_{H_2O}	Mole fraction of water in CO_2 gas phase
x_{CO_2}	Mole fraction of carbon dioxide in water
$K^o_{H_2O}$	Equilibrium constant for solubility of CO_2 in water,
$K^o_{CO_2}$	Equilibrium constant for solubility of water in CO_2
$\overline{V}_{H_2O}$	Average partial molar volume for water in cm^3/mol
$\overline{V}_{CO_2}(gas)$	Average partial molar volume for CO_2 in gas form, cm^3/mol
$\overline{V}_{CO_2}(liq)$	Average partial molar volume for CO_2 in liquid form, cm^3/mol
R	Gas constant which is 83.1447 $bar.cm^3/mol.K$
T	Temperature in Celsius and Kelvin.
ϕ_{CO_2}	Fugacity coefficient for CO_2. Dimensionless.
ϕ_{H_2O}	Fugacity coefficient for H_2O.Dimensionless.
a_{CO_2}	Attraction parameter for pure CO_2. $Bar.cm^6.K^{0.5}.mol^{-2}$
a_{H_2O}	Attraction parameter for pure H_2O.
$a_{H_2O-CO_2}$	Attraction parameter for binary CO_2- H_2O. $Bar.cm^6.K^{0.5}.mol^{-2}$
b_{CO_2}	Repulsion parameter for CO_2.cm^3/mol
b_{H_2O}	Repulsion parameter for H_2O.cm^3/mol
ρ_{H_2O}	Density of water, g/cm^3.